Jurnal Teknologi

Full Paper

BATTERY PERFORMANCE STUDY ON DIFFERENT TYPES OF DRIVING CYCLES FOR ELECTRIC VEHICLE USING MATLAB SIMULINK

Ibrahim Ahmed[a], Mahmoud Saeed[a]*, Khaled Abdel Wahed[a], Essam M. Allam[b], Yasser Fatouh[a]

[a]Faculty of Technology and Education, Helwan University, 4519701 Cairo, Egypt
[b]Faculty of Engineering, Mataria, Helwan University, 11718 Cairo, Egypt

Article history
Received
20 March 2025
Received in revised form
5 August 2025
Accepted
6 August 2025
Published Online
16 June 2026

*Corresponding author
msmrashed2050@gmail.com

Graphical abstract

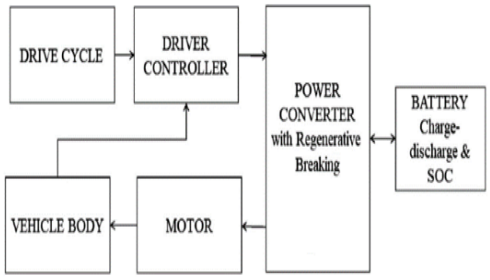

Abstract

Growing concerns regarding fuel consumption and pollutant emissions have accelerated the transition toward electric vehicles (EVs) as an energy-efficient and environmentally sustainable transportation solution. However, battery performance remains strongly influenced by driving conditions, creating challenges for maximizing vehicle range and efficiency. This study investigates the effects of driving cycle variations and road conditions on EV battery performance using a MATLAB-based mathematical model. The developed model simulates different driving scenarios and evaluates battery energy consumption under standard driving cycles, including WLPT, JC08, and UDDS. Results indicate an inverse relationship between road resistance and energy efficiency, where smoother roads reduce battery consumption. Regenerative braking further improves efficiency by recovering braking energy and recharging the battery. Driver behavior showed strong agreement with standard cycles, with WLTP exhibiting the highest average speed and distance (45 km/h and 8.5 km), followed by UDDS (40 km/h and 7.5 km) and JC08 (42 km/h and 7 km). JC08 Hot recorded the highest average voltage (379.988 V) and the lowest current (~7.5 A), indicating stable power demand, whereas WLTP showed the highest current (~9 A). Battery analysis revealed that JC08 Hot had the highest capacity consumption (~3.2 Ah) while maintaining the highest SOC (~98.7%), compared with WLTP, which exhibited a lower SOC (~95.2%). These findings quantitatively demonstrate that improved driving conditions enhance EV energy efficiency, preserve battery charge, and extend vehicle driving range.

Keywords: Driving Cycles, Analysis, Electric vehicle Modeling, State of charge, Lithium-ion batteries

1.0 INTRODUCTION

By 2030, we expect global battery usage to rise fourteen times, with the EU potentially meeting seventeen percent of this demand. Low-carbon transportation, renewable energy, and the growth of the digital economy drive this need mostly. This market will become increasingly significant on a worldwide level as the number of battery-powered electric vehicle models grows. We expect at least thirty million emission-free electric cars to be on EU roads by 2030. Although their batteries harm the natural world, electric cars are supposed to drastically reduce greenhouse gas emissions [1]. Even so, with prices going up right now because of the conflict in Ukraine, it is clear that other energy sources, like hydrogen, will be needed to make the switch to a zero-emission economy easier, since gas and oil imports are still very important [2]. The increasing need for lithium-ion batteries is propelled, in part, by the rising number of people opting for hybrid and electric vehicles. They have undoubtedly become more appealing because of their exceptional qualities, which include great power density, high energy economy, exceptional longevity, and the capacity to function well in partial states of charge (SoC) without requiring constant full charging. However, the energy storage system is the most vital component of an electric powertrain; in fact, designing battery packs for electric vehicles (EVs) continues to be a significant problem in terms of safety, dependability, and system integration. For illustration, thermal runaway from a lithium-ion battery overcharge under poor driving circumstances might result in major fire dangers [3, 4].

A recent study emphasized the importance of accurately estimating the driving range of electric vehicles (EVs), noting that range predictions vary significantly depending on the assessment method used. To address this, the authors developed a mathematical and simulation model within MATLAB/Simulink to evaluate EV power reserve across four widely used driving cycles: NEDC, WLTC, JC08, and US06. The model incorporates vehicle dynamics, resistive forces, and motor efficiency to simulate realistic energy consumption patterns. The study found that the US06 cycle, characterized by high speeds and aggressive acceleration, led to the shortest driving range, while the less dynamic NEDC cycle resulted in a longer range due to its lower acceleration demands. Although JC08 and NEDC showed similar average urban speeds, NEDC provided a longer range due to its inclusion of higher-speed suburban driving phases. The research highlights that low-dynamic cycles contribute to lower energy consumption, but real-world urban EV use often involves more dynamic behavior. Additionally, the study confirmed that frequent braking in urban traffic enables significant regenerative energy recovery. These findings emphasize the value of selecting appropriate driving cycles when modeling EV battery performance, as they offer diverse load profiles that influence energy usage and recovery potential. This is clear from Figures 1, 2, 3, and 4. [5].

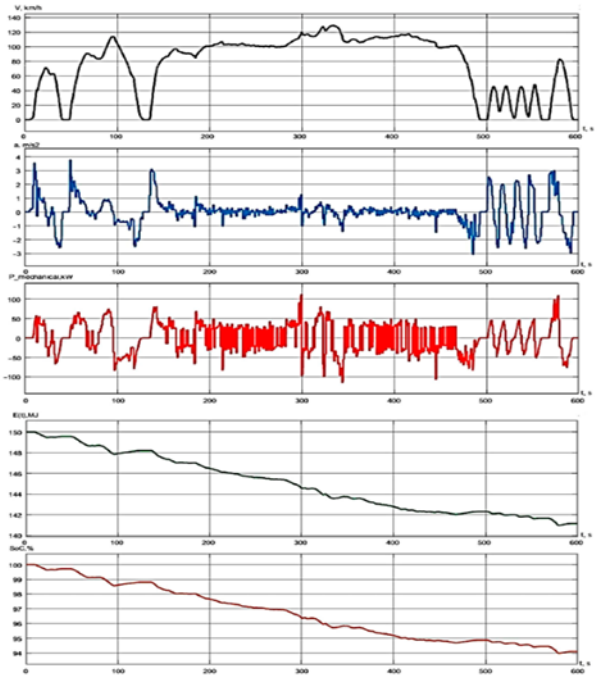

Figure 1 Cycle characteristics US06

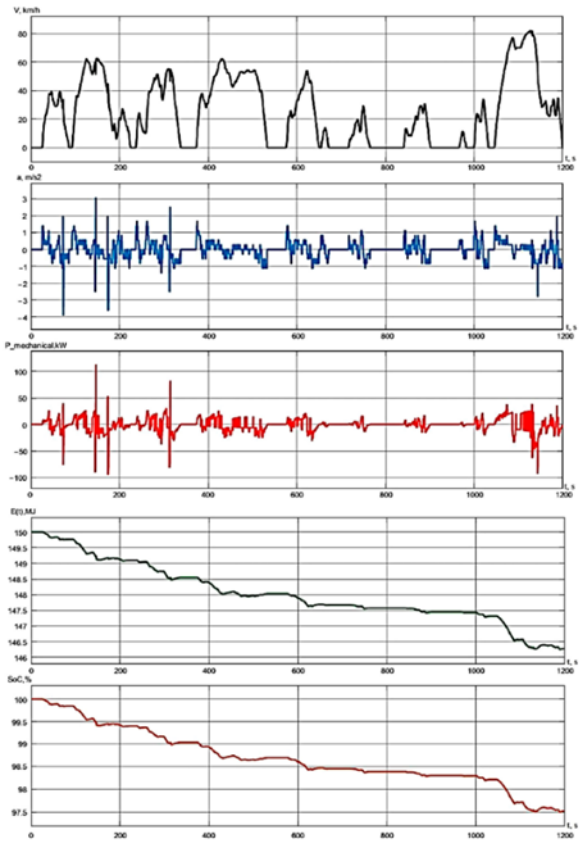

Figure 2 Characteristics of the JC08 cycle

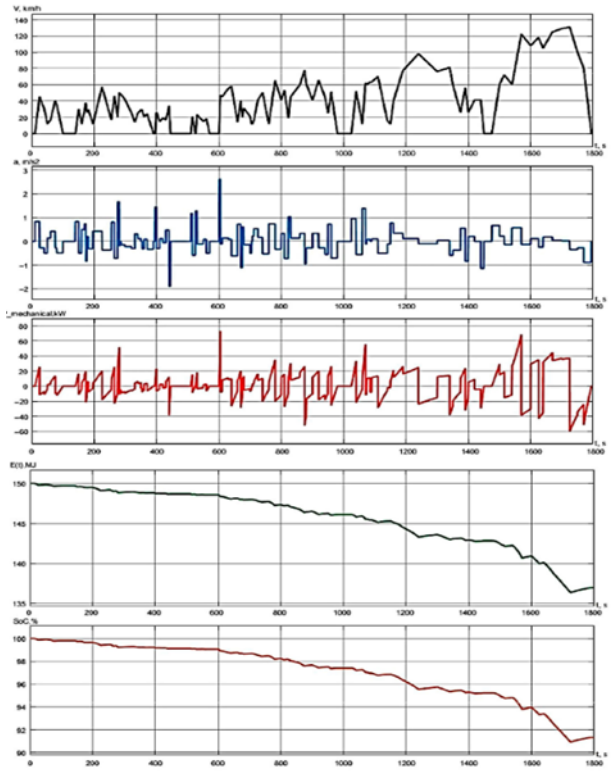

Figure 3 Characteristics of the WLTC cycle

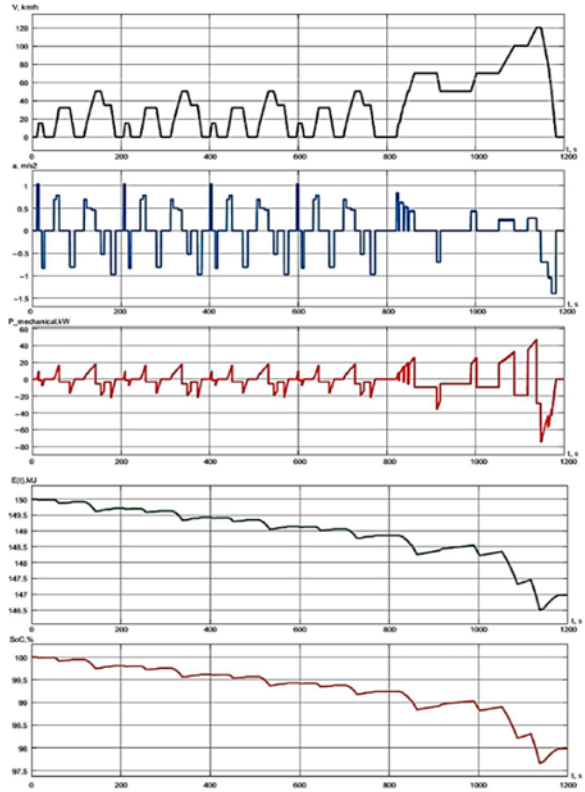

Figure 4 Characteristics of the NEDC cycle

Several studies have utilized MATLAB/Simulink for modeling and simulating electric vehicle (EV) performance, focusing on key subsystems such as the motor, battery, and energy management system to replicate real-world driving conditions. These models allow researchers to assess vehicle dynamics, energy consumption, and powertrain behavior under various standardized driving cycles. Recent simulations have shown that factors such as road surface conditions, driving patterns, and the effectiveness of regenerative braking significantly affect EV performance indicators like acceleration, maximum speed, and battery state-of-charge (SOC). Such simulation tools provide a reliable framework for analyzing EV behavior across different scenarios, aiding in performance comparison, operational planning, and optimizing the strategic placement of charging infrastructure, this is clear from Figures 5, 6, 7, and 8. [6]

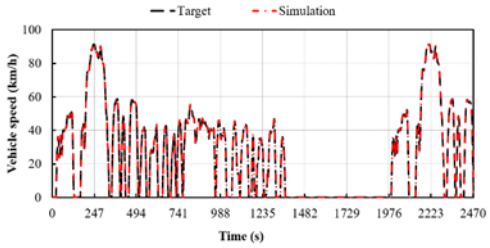

Figure 5 FTP-75 cycle test and simulated vehicle speed

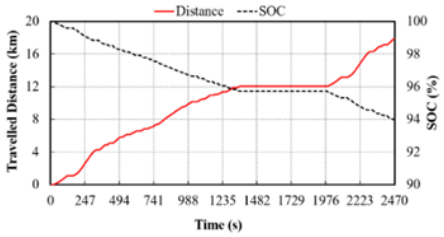

Figure 6 Travelled distance and SOC during FTP-75 cycle test

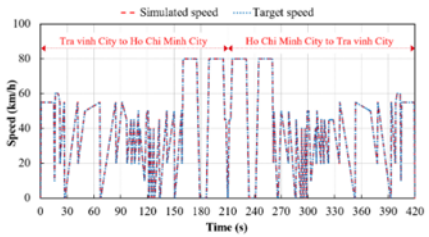

Figure 7 Tra Vinh to Ho Chi Minh city and vice versus cycle test speed

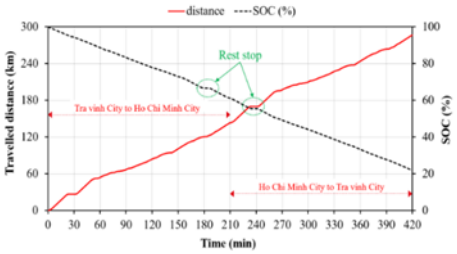

Figure 8 Travelled distance and SOC during the cycle test from Tra Vinh to Ho Chi Minh City and vice versa

A recent study developed a model-based framework to evaluate the battery performance of a two-wheeler electric vehicle drivetrain under various urban driving conditions. Recognizing that the battery pack is one of the most critical and costly components in an EV, the research emphasized the importance of understanding how different driving behaviors—such as aggressive, moderate, and conservative styles—affect battery efficiency and lifespan. The model was validated using standard drive cycles over a simulation duration of 3600 seconds, with each cycle adapted to represent different user driving patterns. This approach provided valuable insights into the influence of real-world driving variability on battery degradation and energy consumption, contributing to improved EV design and energy management strategies, this is clear from Figures 9 and 10. [7]

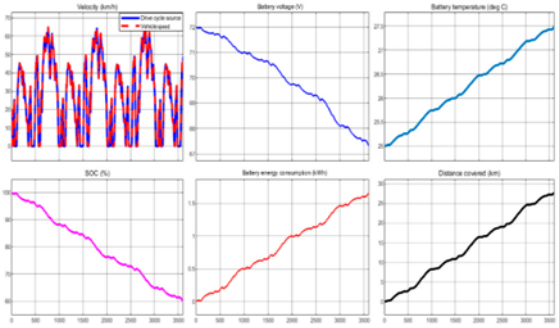

Figure 9 WLTC class 1 drive cycle validation with a two-wheeler EV model and battery performance parameters

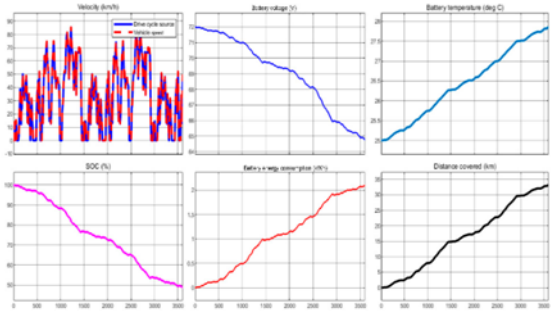

Figure 10 WLTC class 2 drive cycle validation with a two-wheeler EV model and battery performance parameters

Furthermore, it was determined that regulating the temperature of the lithium-ion battery pack is crucial [8]. The range for driving an electric vehicle is contingent upon the designs, dimensions, and kinds of batteries; hence, the battery serves as the principal determinant of the vehicle's cost, size, weight, and execution, in addition to its lifespan, which constitutes a significant constraint of electric vehicles [9].

The study discovered that as a result of repeated cycles of charging and discharging while in operation, the battery grew old with age. Similar to this, a driver's driving style can affect how quickly battery packs age. For example, a ranged driving style can result in more frequent power peaks than a cautious strategy. This will unavoidably start the aging process, which will eventually lead to a steady loss of strength and ability [10]. We note an association between how different physical and chemical phenomena, such as temperature, depth of discharge (DoD), and capacity reduction, are correlated with the causes of performance degradation. and investigated, conducted by the significance of temperature both high and low as an aggravating factor in aging is specifically emphasized. A calendar and cycle ageing study for lithium-ion batteries from several manufacturers is provided with regard to capacity fading and resistance increase. However, because of its non-linear reliance on temperature, charge rate, and state of charge, determining the aging of an electrochemical cell is particularly challenging to comprehend [11].

We have developed an accurate computer-based model to estimate EV electrical consumption under specified driving cycles. We conducted the modeling using MATLAB/Simulink software, adhering to the specifications of the actual vehicle. The model has shown an impressive accuracy in controlling the vehicle's speed in alignment with the driving cycle, achieving results with less than 6% deviation [12]. A robotic driver has been developed to manage vehicle speed in place of a human operator. The robotic driver consisted of linear actuators for the throttle and brake pedals. Subsequently, tests were conducted utilizing the robotic driver while the vehicle was positioned on a chassis on the dynamometer. The findings indicated an improved speed control efficiency [13]. This study addresses the issue of range anxiety among electric vehicle (EV) drivers due to inaccurate remaining range estimation. The paper proposes a hybrid model that combines physics-based models with empirical data to improve the accuracy of power consumption estimation, which in turn enhances remaining range prediction. Data such as power consumption, speed, and road inclination are collected using an onboard monitoring system, and multivariable linear regression is applied to create an accurate power model. The results show that the hybrid model achieves only a 2.52% error, compared to 9.33% in existing models. These improvements can help reduce range anxiety and increase driver confidence in electric vehicles [14,15].

The document gives a thorough look at different mathematical models for electric vehicles (EVs), including simple models with only one degree of freedom (DOF) and more complex models with many bodies moving together. It also discusses dynamic models for various components like the battery, transmission, brakes, and tires, along with a comparative analysis of their applications in controller design. The paper serves as a guide for selecting optimal models for specific EV control design applications [16, 17]. The paper surveys mathematical models for electric vehicles (EVs), from simple single DOF models to complex multi-body dynamics. It discusses dynamic models for key EV components, including the battery, transmission, brakes, and tires, with a focus on their use in controller design. The paper serves as a guide for selecting the most suitable models for EV control applications [18, 19]. The paper explores the potential of electric vehicles (EVs) to reduce fossil fuel use and emissions, addressing environmental issues like air pollution and climate change. It presents a new energy consumption estimation model for EVs under real-world traffic conditions, using positive kinetic energy (PKE) and negative kinetic energy (NKE). The model outperforms existing ones in accuracy, making it highly useful for on-board EV applications [20].

Using data gathered from a smartphone to analyze driving behavior, this research introduces a system that can estimate the remaining charge of an electric vehicle (EV). Researchers found that smartphone data was just as accurate, if not more so, than data collected by onboard equipment. Next, they use a neural network model to predict battery usage based on driving profiles that include factors like speed, acceleration, and jerk. A forecast efficiency of over 95% for projected battery usage was established while testing the system with 10 drivers [21].

This article presents a driving analysis for clustering driving conditions, with data collected in real traffic using advanced vehicle location systems. The study examines the impact of driving on fuel consumption and exhaust emissions through computer simulations, which are then verified by experimental tests. The simulations involve two types of vehicles: a conventional vehicle and an electric vehicle (EV) [22]. A comprehensive review of using driving data and traffic information for reducing vehicle energy consumption. It highlights the innovations and technologies developed in recent decades to decrease energy usage in vehicles. The review concludes that leveraging driving data and traffic information significantly improves energy conservation in vehicles [23].

In this study, a more detailed and application-oriented analysis was presented. This research utilizes a specifically developed and configured MATLAB/Simulink model. The model allows for the addition or replacement of any factor affecting battery performance to simulate and compare the performance of an electric vehicle battery under three widely recognized standard driving cycles: UDDS, JC08 HOT, and WLTP Class 2. The model provides quantitative and graphical results—such as battery consumption in amp-hours and watt-hours/km—under identical time and environmental conditions, such as driver behavior, allowing for a clear numerical comparison between cycles. In addition to the regenerative braking effect, it reveals how smoother surfaces reduce energy consumption and how regenerative braking can usefully recover energy. Additionally, the possibility of replacing the batteries with others with different characteristics is available. A chemical battery system using a lithium-ion NMC (nickel, manganese, cobalt) cell was designed with realistic configurations at 380 volts (96 cells in series), reflecting realistic electric vehicle designs and improving the applicability of the results. Overall, this work not only analyzes performance but also provides practical insights for improving battery efficiency and performance under real-world driving conditions.

2.0 METHODOLOGY

2.1 Modelling of Electric Vehicle and Drive Cycle

The performance of the electric car battery can be evaluated through different driving cycles using a simulation model and performance metrics, which are:
1. Driver behavior: It explains driving the vehicle in all different driving conditions such as: repeated braking, driving at a constant speed, or rapid acceleration.
2. Estimation of the distance traveled (km):
It quantifies the distance traversed by the vehicle over different cycles.
3. Battery Voltage (V):
Tracks the real-time voltage of the battery pack. Stable voltage reflects healthy and efficient battery operation.
4. Battery Current (A):
In EV batteries, the current is changed from positive to negative and vice versa due to charge and discharge cycles, which depend on vehicle acceleration and deceleration and regenerative braking as well.
5. Capacity consumed from battery (Ah):
It indicates how much energy has been drawn from the battery (usually measured in ampere-hours, Ah, or kilowatt-hours, kWh) .It reflects how much energy is used and is influenced by both the driving pattern and the road conditions.
6. State of Charge (SOC) Depletion (%):
Indicates how much charge was used during each cycle. It gives insight into how quickly the battery depletes under different driving conditions.

Figure 11 exhibits a model developed with the vehicle dynamics methodology within the MATLAB Simulink software platform. We employed the velocity profile to ascertain the resistance force, applying fixed blocks for each vehicle parameter. The derivative block's output expended an estimated amount of energy for each instance during a 1320-second simulation.

The drive train basically consists of five components: drive cycles, a lithium-ion battery, an electric motor, and a simple gearbox & differential. As shown in Table 1, the vehicle measurements model sets up a way for sensors and controls to talk to the electric motor controller, the battery controller, and the unit converter. Table 1 summarizes the main components of the developed EV model and their corresponding functions.

The motor's control unit generally oversees the power supplied to the motor, whereas the battery controller is responsible for managing the power produced by the battery.

The battery functions as the exclusive energy storage system, generally employing a lithium-ion cell that provides 380 V and significant current to the power electronics, along with an internal resistance. The power electronics regulate the voltage, current, and frequency to meet the motor's unique demands.

The motor is attached to the vehicle's shaft. The motor is controlled by connecting it to batteries via a power converter. The power converter changes the voltage applied to the motor, which changes the vehicle's speed.

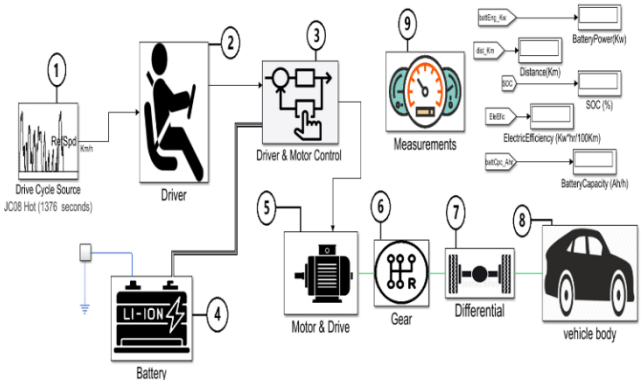

Figure 11 EVs Simulink block Diagram

Table 1 Main components of modelling

No.	Component
1	Drive cycle source
2	Driver
3	Driver & Motor Control
4	Lithium-ion Battery
5	Motor & Drive
6	Gear
7	Differential
8	Vehicle Body
9	Measurements

2.2 Drive Cycles Simulating Driver Behavior

The drive cycle is designed to reflect a standard driving pattern on a global scale. Where in cities and developed countries, driving patterns differ as the majority of the vehicles being driven are made in these countries. Where through the source block of the leadership cycles, different legislative leadership cycles can be used. Driving cycles that cover different parts of the road and different times of day are used in this study. The UDDS and WLTP are the World Harmonized Light Vehicles Test Procedures, respectively, and the Japanese Cycle JC08 that's to compare them and study battery performance on different driving cycles.

Figure 12 represents the Drive Cycle and Driver Behavior Block Diagram. In addition to the different driving behaviors, where can have a significant effect on energy consumption.

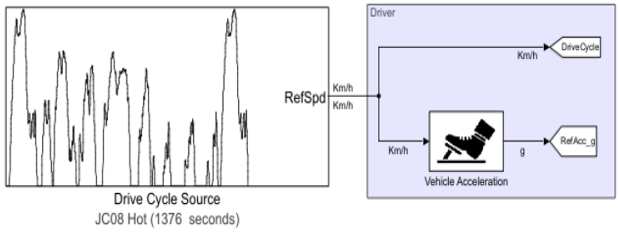

Figure 12 Drive cycle block Diagram

2.3 Vehicle Dynamics

The Vehicle Dynamic block signifies a two-axle vehicle chassis concerning longitudinal movement, as shown in Figure 13. The vehicle can equip its axles with just as many wheels as before or a different total. For instance, the front axle has two wheels, while the rear axle only has one. The premise is that the vehicle's wheels maintain a consistent size throughout. Anywhere on or below the vehicle's path of travel might be its center of gravity (CG).

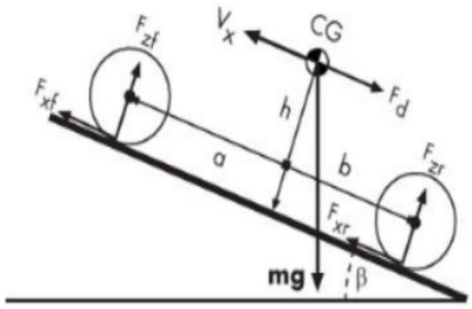

Figure 13 The Vehicle Dynamics and Motion forces analysis

The overall influence of all forces and torques acting on the vehicle dictates its movement. The forces that act along the length of the tires are responsible for the vehicle's movement in either the forward or backward direction. The center of gravity (CG) represents the location where the vehicle's mass is effectively concentrated. Depending on the angle of inclination, the vehicle's weight draws it towards the ground, causing it to move either forward or backward. The vehicle experiences a decrease in speed due to aerodynamic drag, regardless of whether it is moving forward or backward. The drag is assumed to act through the CG for simplicity.

Vehicle Dynamics and Motion forces analysis, the following equations explain this [18]:

$$(1) \quad m \cdot v_x = F_x - F\_d - mg \cdot \sin(\beta)$$

This represents the equation of motion in the longitudinal direction (x-axis).
- v_x: Rate of change of longitudinal velocity
- m Mass of vehicle
- g Gravitational acceleration
- F_x: Driving force from the wheels
- F_d: Air resistance force (aerodynamic)
- mg·sin(β): The component of the effective weight acting on the incline.

$$(2) \quad F_x = n(F_xf + F_xr)$$

The total longitudinal force resulting from the front and rear wheels.
- F_xf, F_xr: Forces acting on the front and rear wheels
- n: Power distribution coefficient (or number of engines)

$$(3) \quad F\_d = \tfrac{1}{2} \cdot c\_d \cdot \rho\_a \cdot (v_x + v\_w)^2$$

Air resistance equation.
- c_d: Drag coefficient
- ρ_a: Air density
- v_w: Wind speed
- v_x + v_w: Relative air speed

$$(4) \quad F\_zf = [\, -h(F\_d + mg \cdot \sin(\beta) + m \cdot v_x) + b \cdot mg \cdot \cos(\beta) \,] \,/\, (n(a + b))$$

Represents the distribution of vertical load on the front wheels.
- F_zf: Vertical force on the front wheels
- h: Height of the center of mass
- a, b: The distance between the center of mass and the front and rear axles.

$$(5) \quad F\_zr = [\, +h(F\_d + mg \cdot \sin(\beta) + m \cdot v_x) + a \cdot mg \cdot \cos(\beta) \,] \,/\, (n(a + b))$$

Represents the distribution of vertical load on the rear wheels.
- F_zr: Normal force on the rear wheels

$$(6) \quad F\_rr = C\_rr \times m \times g \times \cos(\beta)$$

- F_rr: Rolling resistance force
- C_rr: Rolling resistance coefficient (≈0.01 to 0.015 depending on road and tire type)
- m: Mass
- g: Gravity
- β: Road inclination angle

$$(7) \quad F\_acc = m \times a_x$$

- F_acc :Inertial Resistance
- a_x: Longitudinal acceleration = dv_x/dt

$$(8) \quad F\_total = F\_d + F\_rr + F\_acc + mg \cdot \sin(\beta)$$

- F_total: Total Tractive Effort

2.4 Lithium-ion Battery

As the battery's current fluctuates over time, the phrase "state-of-charge" (SOC) is used to represent the terminal voltage equation during discharge and the charge content in the battery. SOC inertia refers to the starting state of the charge level, whereas Q tot (Ah) denotes the entire charge capacity of the battery. A lithium-ion battery cell typically has defined maximum and minimum terminal voltage levels, as well as specified maximum and minimum current limits, or C-rates. If the discharge rate is 1C, the current is enough to deplete the battery entirely within one hour. A continuous current discharge at a C/3 rate is typically used to assess a battery's energy capacity. The output power might also be constrained by a minimum voltage requirement.

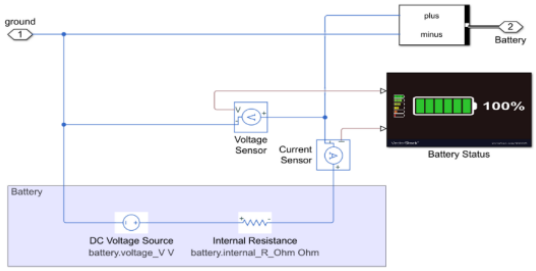

Figure 14 This is a simple battery model that features a distinct internal resistance for discharge, and it is designed to work alongside the battery Simulink block

Battery Model Description:

The electric vehicle battery system is modeled using Lithium-Ion NMC (Nickel Manganese Cobalt) cell chemistry, known for its high energy density, good thermal performance, and long cycle life — making it a common choice in EV applications.

Cell Specification: Each lithium-ion cell used in the model has a nominal voltage of 3.7V and a capacity of 50Ah.
Battery Pack Configuration: The pack consists of 103 cells connected in series (103s1p), resulting in a nominal pack voltage of approximately 380V and a total energy capacity of 19 kWh.
Modeling Level: The simulation is conducted at the pack level, where the voltage-SOC relationship and power consumption are modeled using an equivalent circuit approach.

Battery Specifications:
- Total Voltage: 380 V (from 96 cells × 3.96 V nominal per cell)
- Cell Configuration: 96s20p (96 cells in series × 20 cells in parallel)
- Cell Capacity: Approximately 3.5 Ah
- Total Capacity: 3.5 Ah × 20 = 70 Ah
- Total Energy: 380 V × 70 Ah = 26.6 kWh

2.5 Permanent Magnet Synchronous Motor PMSM

Permanent Magnet Synchronous Motors (PMSMs) are similar to three-phase induction motors in operation. The three-phase voltage source linked to the stator winding generates a rotating magnetic field (RMF). The RMF induces rotation of the rotor. The Permanent Magnet Synchronous Motor (PMSM) has zero rotor-side power losses because it uses a permanent magnet within its rotor. This machine is capable of delivering a consistent torque output. The Figure 15 illustrates the configuration and equivalent circuit of the PMSM.

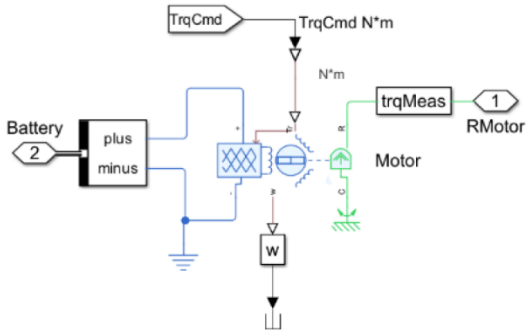

Figure 15 Steady state model of a PMSM and the Motor & Drive Simulink block

This block is meant to look like a brushless motor and drive system, such as a Permanent Magnet Synchronous Motor (PMSM). It can also be used to simulate other types of motors used in traction and actuation systems. This assembly integrates the motor, drive electronics, and control systems to enable efficient system-level simulation. The torque speed envelope defines the range of torques and speeds that the block allows.

2.6 Gear Box and Differential

At Figure 16, the gearbox—a simple gear block—constrains the connected drive line axes of the base gear, B, and the follower gear, F, to coordinate with the certain ratio you demonstrate. You may specify whether the follower axis operates in a different or identical way as the base axis.

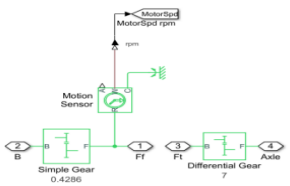

Figure 16 Gearbox & Differential Simulink block

The above discussion proposes that batteries are the vehicle's only stored energy system. So, the batteries generate the electricity essential for driving the vehicle. Batteries, on the opposite hand, get charged employing energy from motion acquired through regenerative braking processes.

The above simulation determines the amount of capacity required or created throughout the driving cycle, the charge level of the battery and current of discharge, and the battery's amount of charge.

3.0 RESULTS AND DISCUSSION

3.1 Drive Cycles Simulating Driver Behavior

As shown in Figures 17, 18, and 19, a significant alignment of the driver's behavior with the driving cycle in order at a unified time period from 0 to 1320 seconds to achieve more realistic results.

These figures compare standardized driving cycles (WLPT Class 2, JC08 Hot, and UDDS) with actual driver speed profiles over time, serving as a key validation step to ensure that the selected cycles accurately represent real-world driving behavior in EV battery performance simulations.

The WLPT Class 2 cycle (orange) shows strong alignment with the actual driver speed profile (green), indicating its effectiveness in representing real-world driving behavior on the tested route. This confirms its reliability for simulating battery load, energy consumption, and thermal effects, particularly in urban or suburban conditions under hot climates.

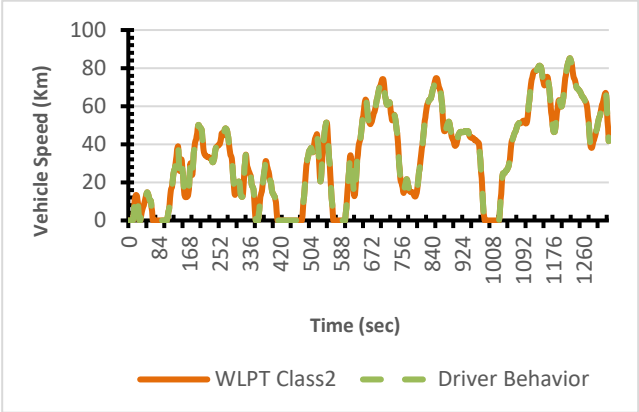

Figure 17 Comparison between the driving cycle WLPT class2 and the driver's behavior

The JC08 Hot cycle (blue) closely mirrors real driver behavior (green), with only slight differences during rapid acceleration or braking, reflecting natural human variability. Despite these minor deviations, it effectively simulates battery charge-discharge patterns and regenerative braking in warm climate conditions, making it a reliable representation for typical Asian driving scenarios.

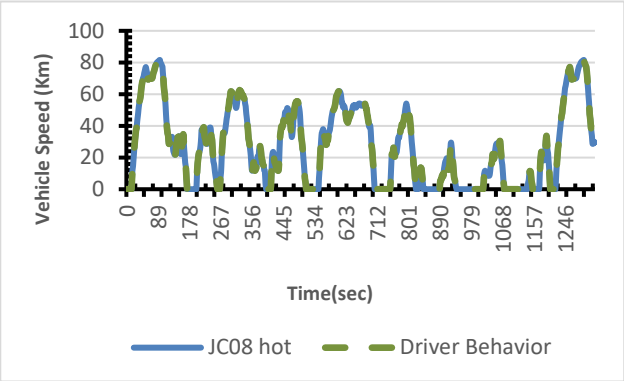

Figure 18 Comparison between the driving cycle JC08 hot and the driver's behavior

The UDDS cycle (black) shows a fair alignment with the actual driver speed profile, though it diverges more in speed variability and stop durations compared to other cycles. This suggests it may not fully capture the effects of aggressive or frequent stop-and-go driving on battery performance. However, it remains a valuable standard for regulatory testing and energy consumption evaluation

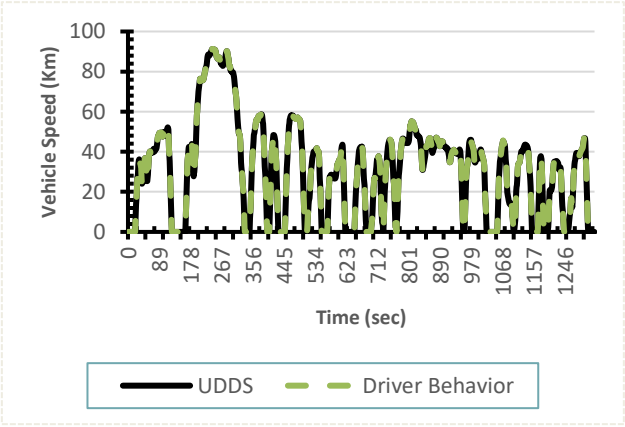

Figure 19 Comparison between the driving cycle UDDS and the driver's behavior

Figure 20 illustrates the mean vehicle speed across three standard driving cycles: WLPT Class 2, JC08 HOT, and UDDS. The WLPT Class 2 cycle recorded the highest mean speed, approximately 35 km/h, followed closely by the UDDS cycle at around 32 km/h, while the JC08 HOT cycle showed the lowest mean speed of about 28 km/h. These differences highlight the varying nature of driving patterns in each cycle. The lower average speed in JC08 HOT reflects more frequent stops and slower acceleration phases, typical of urban traffic in warm regions. In contrast, WLPT Class 2 and UDDS cycles involve smoother acceleration and fewer stops, allowing for higher mean speeds. These speed variations directly influence battery performance, as higher average speeds tend to increase energy consumption, while slower, stop-and-go patterns can enhance regenerative braking opportunities but may also raise current draw during frequent acceleration.

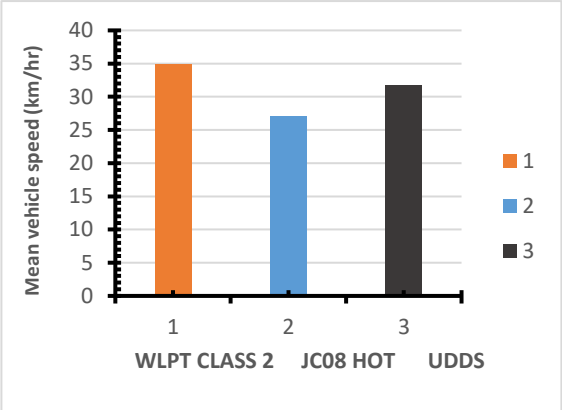

Figure 20 The Mean vehicle speed on three drive cycle

This research emphasizes the importance of comparing real-world driving behavior with standardized driving cycles (WLPT Class 2, JC08 HOT, and UDDS) to validate simulation accuracy. Figures 17, 18, and 19 confirm that these cycles realistically represent driver speed patterns, ensuring that battery performance predictions—such as energy consumption, regenerative braking efficiency, and state of charge (SoC) fluctuations—are reliable. Accurate speed-time inputs improve the credibility of energy use estimates (kWh/km), reflect actual deceleration for regenerative braking calculations (with up to 10–15% energy recovery), and capture realistic SoC dynamics critical for battery aging and thermal management analysis. This strengthens the generalizability of the findings and supports the robustness of the battery model under various real-world driving conditions.

3.2 Travelled Distance

The Figures 21 illustrates the relationship between distance and time for three driving cycles—WLPT Class 2, JC08 HOT, and UDDS—highlighting how vehicle movement varies with each profile. The WLPT Class 2 cycle covers the greatest distance at 13.15 km, followed by UDDS at 12 km, and JC08 HOT at 10.21 km. These variations reflect differences in speed, acceleration, and stop frequency across the cycles, offering insights into how driving patterns influence travel efficiency over time. And we note that the distance travelled in the driving cycle WLPT Class 2 is much greater than the other two driving cycles in order to increase the speed of the car in this cycle.

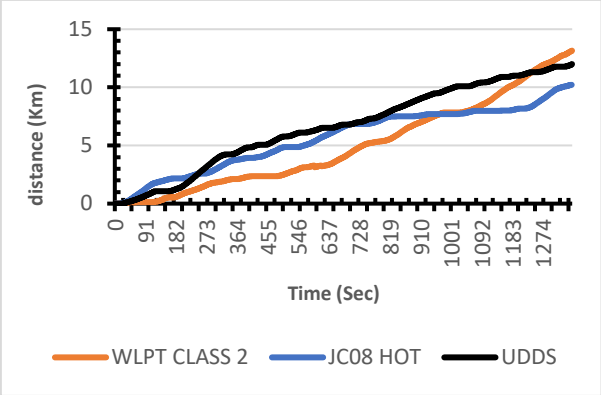

Figure 21 Relationship between Distance traveled and Time

Figure 22 presents the mean distance traveled for each of these three driving cycles, providing a summarized value of average distance covered during the test period for each cycle.

Figure 22 The mean Distance traveled on three drive cycle

Figures 21 and 22 are closely related, with Figure 21 showing the time-based progression of distance traveled for each driving cycle, and Figure 22 summarizing this data as mean distances. The steeper slope of the WLPT Class 2 curve in Figure 21 reflects higher average speeds and fewer stops, resulting in the highest mean distance (~8 km) in Figure 22. In contrast, the UDDS and JC08 HOT cycles show flatter slopes and lower mean distances (~6.7 km and ~5.8 km), indicating slower speeds and more frequent stops. Together, these figures provide both detailed and summarized insights into how driving patterns affect travel efficiency, battery consumption, and overall EV performance.

3.3 Battery Voltage

Voltage expresses the thrust of electrons through the circuit where changes in voltage depend on the slowdown and speed of the vehicle and the range of the state of charge.

Figure 23 illustrates the effect of each drive cycle on the input voltage of the three phase AC motor of the electric vehicle during its movement at time 0 to 1320 second

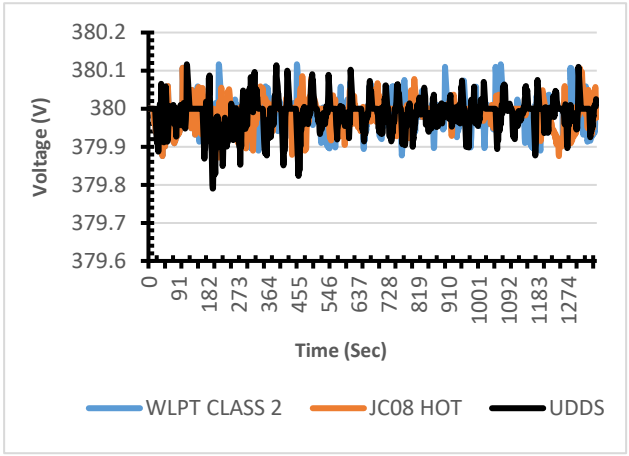

Figure 23 the effect of drive cycle on the input Voltage of the electric motor

Figure 24 shows the effect of the three drive cycles on the input mean voltage of the three-phase motor the results showed that the three drive cycles had no significant effect on the mean input voltage to the electric motor which is 380 volts approximately

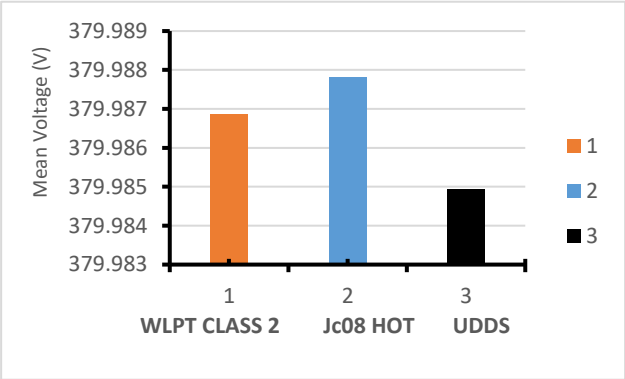

Figure 24 the input mean voltage of the electric motor

3.4 Battery Current

As known, current is the rate at which electric charge passes through a circuit. In EV batteries, the current is changed from positive to negative and vice versa due to charge and discharge cycles, which depend on vehicle acceleration and deceleration and regenerative braking as well. In figure 25 it is noticed that the amount of drained current is high on drive cycle WLPT CLASS2 due to the high speed and no stopping distance, and almost the speed is stable.

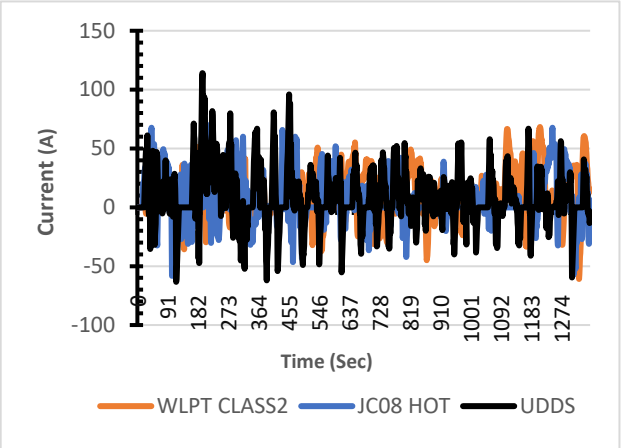

Figure 25 the effect of drive cycle on the input current of the electric motor

Figure 26 shows us that the current consumed in the driving cycle Jc08 HOT is less than the other two driving cycles because of the stopping distances are long of

The drive cycle the amount of electricity consumed in the electric motor in the Jc08 HOT driving cycle is smaller than the two other driving cycles, which are WLPT class 2 and UDDS, and this may be due to resistances that meet the vehicle in WLPT class 2 and UDDS more than the road resistance in Jc08 HOT road it and has more stopping distances for charging. The corresponding resistances of the vehicle, such as rolling resistance, air resistance, acceleration resistance, and hill climbing resistance, may be the reason for higher consumption in the WLPT class 2 and UDDS driving cycles than in the JC08 Hot driving cycle

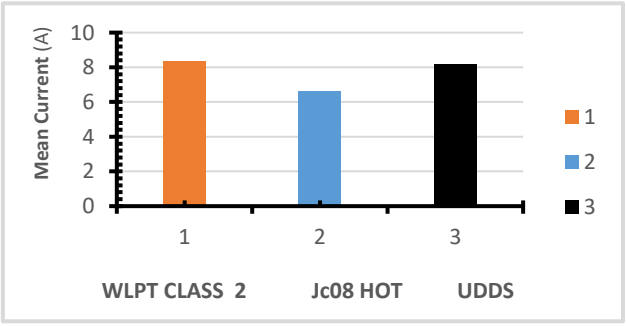

Figure 26 the input mean current of the electric motor

3.5 Capacity consumed from battery

Capacity is the total profit of power produced through electrochemical operations within the battery, expressed in ampere hours.

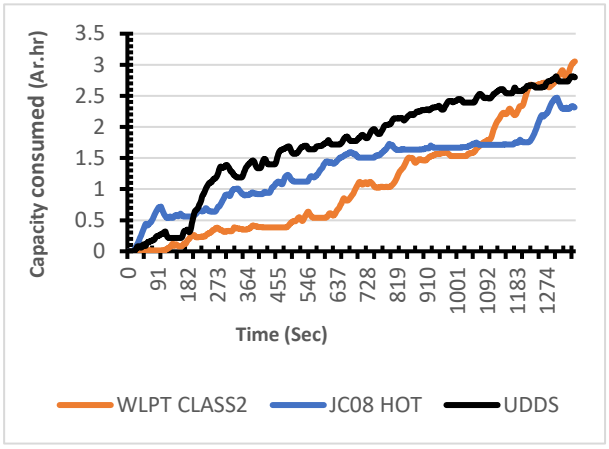

Figure 27 Relationship between Capacities consumed and time on the three drive cycle

The size of the battery defines the optimum torque of the electric motor and also the vehicle's range and weight. Limiting battery storage capacity while retaining motor power decreases vehicle range.

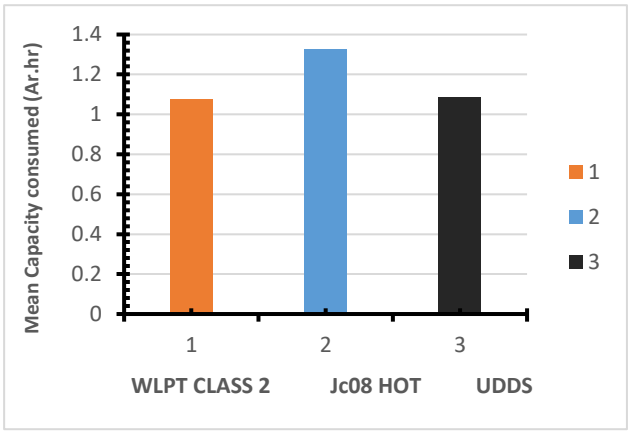

Figure 28 the mean Capacity consumed on the three drive cycle

Additional useful knowledge that we can deduce from the above comparison is that the vehicle range does not only depend on the capacity of the battery but also on the driving mode for WLPT CLASS UDDS. The results are almost equal, but it is not the case in JC08HOT. Furthermore, selecting a proper battery pack size will boost the range of a vehicle running on electricity.

3.6 State of charge

The state of charge (SOC) of a battery is the quantity of energy readily available at a specific moment in time, constituted as a percentage. The research results show that the SoC declines overall, with only a few examples of it boosting in between, which is due to the regenerative braking system. As mentioned earlier, regenerative braking assures that as the vehicle declines, the kinetic energy goes back to the battery, where the motor operates like a source of energy.

Figures 29 and 30 together illustrate how the State of Charge (SOC) of the battery changes over time under different driving cycles and provide insight into the overall battery energy efficiency for each cycle.

Figure 29 – Time-Based SOC Trend: This figure shows the real-time decrease in SOC (%) throughout the driving cycles: WLPT Class 2, JC08 HOT, and UDDS. - The UDDS cycle shows the steepest decline, indicating the highest energy consumption and most demanding profile on the battery. - WLPT Class 2 demonstrates a moderate drop, suggesting a balanced energy demand. - JC08 HOT has the least SOC decline, reflecting the most efficient energy usage during that cycle.

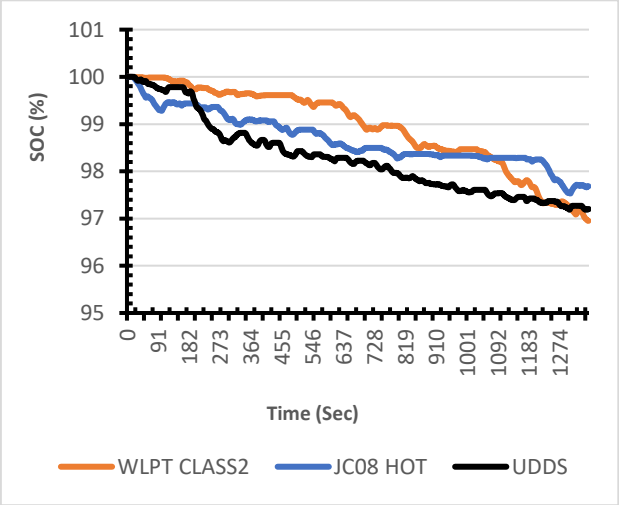

Figure 29 Relationship between SOC present in the battery and time on the three drive cycle

Figure 30 – Mean SOC Comparison: This figure summarizes the average SOC across the entire duration of each drive cycle. - JC08 HOT retains the highest average SOC, confirming lower battery depletion. - WLPT Class 2 and UDDS show lower mean SOC values, aligning with the sharper declines observed in Figure 29.

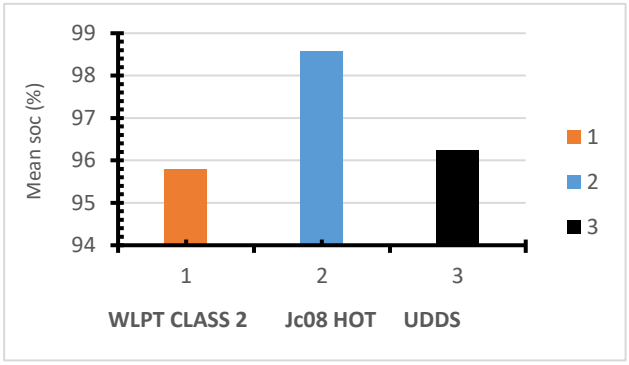

Figure 30 The mean SOC present in the battery on the three drive cycle

The two figures are complementary—Figure 29 captures dynamic SOC behavior over time, while Figure 30 provides a cumulative metric for easier comparison. Together, they confirm that JC08 HOT is the most battery-efficient cycle, while UDDS is the most energy-consuming, largely due to its aggressive acceleration and frequent stop-go patterns. This analysis is essential for optimizing drive strategies and evaluating battery performance under real-world scenarios.

4.0 CONCLUSION

In this study, comprehensive simulations were used to investigate how an electric vehicle battery responds under different driving cycle conditions.

Among the various driving cycles tested, the WLTP Class 2 cycle exhibited the highest energy consumption, despite all driving cycles having the same test duration of 1320 seconds. This emphasizes the significant influence of the driving profile on battery performance and the amount of energy consumed through sudden acceleration and drawing a larger electrical current, which generates more heat and affects battery performance. The simulation revealed that the lower the energy losses resulting from the road, the less energy is consumed by the battery.

Future studies will focus on extending this analysis to real-world driving conditions on privately modeled roads in Egypt, which will help further understand how local road conditions and driving behaviors impact EV performance and energy efficiency.

Acknowledgement

I would like to demonstrate my deep gratitude to my supervisors. (Professor Ibrahim Ahmed, Khaled Abdel Wahed, Essam M. Allam, and Yasser Fatouh) for throughout my academic journey, they consistently supported me and supplied me with valuable suggestions, and their tireless commitment to doing

excellent in educational institutions and their meticulous focus on detail have had an important effect on the subject of this dissertation.

Conflicts of Interest

The authors declare that there is no conflict of interest regarding the publication of this paper.

References

[1] European Parliament. 2021. *New EU Regulatory Framework for Batteries Setting Sustainability Requirements*. Brussels: European Parliament. Accessed [date accessed]. Available online: https://www.europarl.europa.eu/RegData/etudes/BRIE/2021/689337/EPRS_BRI(2021)689337_EN.pdf.

[2] Hume, Neil, Emiko Terazono, and Tom Wilson. 2022. European Gas Prices Soar and Oil Tops $105 after Russia Attacks Ukraine. *Financial Times*. Available online: https://www.ft.com/content/c6303127-5edf-4256-9c25-effa75766002.

[3] Duh, Y.-S., Y. Sun, X. Lin, J. Zheng, M. Wang, Y. Wang, X. Lin, X. Jiang, Z. Zheng, S. Zheng, *et al.* 2021. Characterization on Thermal Runaway of Commercial 18650 Lithium-Ion Batteries Used in Electric Vehicles: A Review. *Journal of Energy Storage*. 41: 102888. https://doi.org/10.1016/j.est.2021.102888.

[4] Duh, Y.-S., J.-H. Theng, C.-C. Chen, and C.-S. Kao. 2020. Comparative Study on Thermal Runaway of Commercial 14500, 18650 and 26650 LiFePO4 Batteries Used in Electric Vehicles. *Journal of Energy Storage*. 31: 101580. https://doi.org/10.1016/j.est.2020.101580.

[5] Martyushev, Nikita V., Boris V. Malozyomov, Svetlana N. Sorokova, Egor A. Efremenkov, and Mengxu Qi. 2023. Mathematical Modeling the Performance of an Electric Vehicle Considering Various Driving Cycles. *Mathematics*. 11(11): 2586. https://doi.org/10.3390/math11112586.

[6] Banh, Huynh Thanh, and Thach Ngoc Phuc. 2025. Dynamic Model Development and Automotive Dynamics Simulation Utilizing Matlab/Simulink. *International Journal of Research and Scientific Innovation*. https://doi.org/10.51244/IJRSI.2025.12040056.

[7] Lakshmanan, Padmavathi, Anand Abhishek, Brijendra Kumar Verma, and Subhash Kumar Ram. 2024. Performance Assessment of Two-Wheeler Electric Vehicle Batteries Using Multi-Mode Drive Cycles. *World Electric Vehicle Journal*. 15(4): 145. https://doi.org/10.3390/wevj15040145.

[8] Verma, A., and D. Rakshit. 2022. Performance Analysis of PCM-Fin Combination for Heat Abatement of Li-Ion Battery Pack in Electric Vehicles at High Ambient Temperature. *Thermal Science and Engineering Progress*. 32: 101314. https://doi.org/10.1016/j.tsep.2022.101314.

[9] Laoonual, Yossapong. 2013. *Assessment of Electric Vehicle Technology Development and Its Implication in Thailand*. Bangkok: King Mongkut's University of Technology Thonburi and National Metal and Materials Technology Center.

[10] Eboli, Laura, Gabriella Mazzulla, and Giuseppe Pungillo. 2017. How Drivers' Characteristics Can Affect Driving Style. *Transportation Research Procedia*. 27: 945–952. https://doi.org/10.1016/j.trpro.2017.12.024.

[11] Gailani, A., R. Mokidm, M. El-Dalahmeh, M. El-Dalahmeh, and M. Al-Greer. 2020. Analysis of Lithium-Ion Battery Cells Degradation Based on Different Manufacturers. In *Proceedings of the 55th International Universities Power Engineering Conference (UPEC 2020)*, Turin, Italy, September 1–4, 2020. https://doi.org/10.1109/UPEC49904.2020.9209759.

[12] Svens, P., A. J. Smith, J. Groot, M. J. Lacey, G. Lindbergh, and R. W. Lindstrom. 2022. Evaluating Performance and Cycle Life Improvements in the Latest Generations of Prismatic Lithium-Ion Batteries. *IEEE Transactions on Transportation Electrification*. 8: 3696–3706. https://doi.org/10.1109/TTE.2022.3158838.

[13] Miri, I., A. Fotouhi, and N. Ewin. 2021. Electric Vehicle Energy Consumption Modelling and Estimation: A Case Study. *International Journal of Energy Research*. 45(1): 501–520. https://doi.org/10.1002/er.5700.

[14] Hong, J., S. Park, and N. Chang. 2016. Accurate Remaining Range Estimation for Electric Vehicles. In *Proceedings of the Asia and South Pacific Design Automation Conference (ASP-DAC 2016)*, 781–786. January 25–28, 2016. https://doi.org/10.1109/ASPDAC.2016.7428106.

[15] Lekshmi, S., and P. S. Lal Priya. 2019. Mathematical Modeling of Electric Vehicles: A Survey. *Control Engineering Practice*. 92: 104138. https://doi.org/10.1016/j.conengprac.2019.104138.

[16] Diaz Alvarez, A., F. Serradilla Garcia, J. E. Naranjo, J. J. Anaya, and F. Jimenez. 2014. Modeling the Driving Behavior of Electric Vehicles Using Smartphones and Neural Networks. *IEEE Intelligent Transportation Systems Magazine*. 6(3): 44–53. https://doi.org/10.1109/MITS.2014.2322651.

[17] Wang, Jiquan. 2016. *Battery Electric Vehicle Energy Consumption Modelling, Testing and Prediction: A Practical Case Study*. Eindhoven: Technische Universiteit Eindhoven.

[18] Moure, C., M. Roche, and M. Mammetti. 2014. Range Estimator for Electric Vehicles. In *2013 World Electric Vehicle Symposium and Exhibition (EVS27)*. 1–15. https://doi.org/10.1109/EVS.2013.6914917.

[19] Pan, C., W. Dai, L. Chen, L. Chen, and L. Wang. 2017. Driving Range Estimation for Electric Vehicles Based on Driving Condition Identification and Forecast. *AIP Advances*. 7(10): 105206. https://doi.org/10.1063/1.4993945.

[20] Qi, X., G. Wu, K. Boriboonsomsin, and M. J. Barth. 2018. Data-Driven Decomposition Analysis and Estimation of Link-Level Electric Vehicle Energy Consumption under Real-World Traffic Conditions. *Transportation Research Part D: Transport and Environment*. 64: 36–52. https://doi.org/10.1016/j.trd.2017.08.008.

[21] Diaz Alvarez, A., F. Serradilla Garcia, J. E. Naranjo, J. J. Anaya, and F. Jimenez. 2014. Modeling the Driving Behavior of Electric Vehicles Using Smartphones and Neural Networks. *IEEE Intelligent Transportation Systems Magazine*. 6(3): 44–53. https://doi.org/10.1109/MITS.2014.2322651.

[22] Montazeri-Gh, M., A. Fotouhi, and A. Naderpour. 2011. Driving Patterns Clustering Based on Driving Feature Analysis. *Proceedings of the Institution of Mechanical Engineers, Part C: Journal of Mechanical Engineering Science*. 225(6): 1301–1317. https://doi.org/10.1177/2041298310392599.

[23] Fotouhi, A., R. Yusof, R. Rahmani, S. Mekhilef, and N. Shateri. 2014. A Review on the Applications of Driving Data and Traffic Information for Vehicles' Energy Conservation. *Renewable and Sustainable Energy Reviews*. 37: 822–833. https://doi.org/10.1016/j.rser.2014.05.077.